Authors' version.

Published in:

IEEE TRANSACTIONS ON BIOMEDICAL ENGINEERING, VOL. 56, NO. 3, MARCH 2009

Digital Object Identifier : 10.1109/TBME.2008.2005584

Valentina Agostini[1], Marco Knaflitz[1], *Member, IEEE*, Filippo Molinari[1], *Member, IEEE*

[1]Dip. Elettronica, Politecnico di Torino, Corso Duca degli Abruzzi 24, 10129 Torino, Italy

Motion artifact reduction in breast dynamic infrared imaging

Abstract — Dynamic infrared imaging is a promising technique in breast oncology. In this study a QWIP infrared camera is used to acquire a sequence of consecutive thermal images of the patient's breast for 10 s. Information on the local blood perfusion is obtained from the spectral analysis of the time series at each image pixel. Due to respiratory and motion artifacts, the direct comparison of the temperature values that a pixel assumes along the sequence becomes difficult. In fact, the small temperature changes due to blood perfusion, of the order of 10-50 mK, which constitute the signal of interest in the time domain, are superimposed onto large temperature fluctuations due to the subject's motion, which represent noise. To improve the time series signal-to-noise ratio, and, as a consequence, enhance the specificity and sensitivity of the dynamic infrared examination, it is important to realign the thermal images of the acquisition sequence thus reducing motion artifacts. In a previous study we demonstrated that a registration algorithm based on fiducial points is suitable to both clinical applications and research, when associated with a proper set of skin markers.

In this paper, we quantitatively evaluate the performance of different marker sets by means of a model that allows for estimating the signal-to-noise ratio increment due to registration, and we conclude that a

12-marker set is a good compromise between motion artifact reduction and the time required to prepare the patient.

Index Terms— Breast cancer detection, dynamic infrared imaging, image registration, signal-to-noise ratio estimation, skin markers, thermal image sequence.

I. INTRODUCTION

Dynamic Area Telethermometry (DAT) has been proposed as a new imaging modality for improving breast cancer diagnosis [1-3] and for assessing the response to systemic therapy [4]. DAT is harmless, noninvasive, and does not expose the subject to ionizing radiations. It allows observing skin temperature fluctuations in the range of a few tens of millikelvin, which reportedly are influenced by spatial and temporal abnormalities in blood perfusion of the observed tissues. These abnormalities are due to presence of cancer-associated extra-vascular nitric oxide [1-2], to the specific characteristics of the vasculature supplying blood to the tumor and to the altered metabolism of cancerous tissue. Thermal image sequences are generally acquired by using last generation high resolution infrared thermographs [5].

DAT examination requires the acquisition of a sequence of consecutive thermal images with a rate ranging from 50 frames/s up to 200 frames/s, during an observation window lasting a few tens of seconds. Clinical information is obtained by analyzing in the frequency domain the small temperature fluctuations taking place in numerous breast areas constituted by a few pixels, rather than considering the classical static, color-coded bitmap of the skin temperature, namely the thermogram, which is often difficult to interpret [6].

During the acquisition of the infrared sequence, the patient's breast moves non-rigidly due to physiological (breathing, heart activity, …) and random movements. These movements, associated with

the thermal gradients of the observed skin surface, generate artifactual fluctuations of the local temperature that, in turn, act as noise superimposed onto the temperature fluctuations to be studied.

Therefore, before proceeding with the harmonic analysis, it is fundamental to geometrically realign all the thermograms constituting the sequence with respect to a reference one. This registration procedure allows attenuating the motion artifacts by reducing local movements to fractions of a pixel, and, consequently, it allows improving the signal-to-noise ratio of the signals to be processed [7].

Registration procedures may be classified either as marker-based or marker-less [8].

Marker-less procedures require that images have sharp features, which can allow for segmentation and landmark identification. Unfortunately, marker-less procedures are challenging tasks in human thermograms [9-10], due to the absence of sharp and well-contrasted natural features and to the presence of intensity changes between images belonging to the dynamic sequence.

Previous experience showed that marker-based registration procedures are preferable in this application for the specific characteristics of breast infrared images. The number of markers, the ease of positioning, and the positioning repeatability are crucial characteristics of a marker set suitable for clinical use. Moreover, the marker set must warrantee a sufficient attenuation of motion artifacts after registration and, correspondingly, a sufficient increment of the signal-to-noise ratio.

This paper shows that a set consisting of 12 markers gives results similar to those obtained by using 18 markers, while by reducing the number of markers to 7 or less the effectiveness of the registration procedure is significantly compromised in terms of increment of the signal-to-noise ratio.

II. Materials and methods

A. Data acquisition

The infrared image sequences were acquired with an AIM256Q camera (Long Wave Quantum Well Infrared Photodetector, produced by AEG Infrarot-Module GmbH) having a NETD equal to 17.3 mK at 300 K, with an integration time equal to 20 ms. The acquisition time was equal to 10 s and the frame rate

was 50 frames/s. Hence, each sequence consisted of 500 thermal images with a dynamic range of 14 bit. The field-of-view was 38 cm × 38 cm, with a matrix of 256×256 pixels and hence a pixel size of approximately 1.5 mm. A two-point calibration of the infrared camera was performed before each acquisition.

Twenty healthy women, with age ranging from 22 to 72 years and breast size ranging from cup A to cup DD, were enrolled in this study. The preparation of the patient and the exam were carried out following the indications of the protocol approved by the ethical committee of Ospedale Molinette di Torino (Italy). Patients were asked to lie down onto an examination table with a backrest inclination of 40 degrees with respect to the horizontal plane. They were also asked to raise their arms with the hands resting over their head.

We acquired a frontal view of the subjects comprehending both breasts. The optical axis of the infrared camera was perpendicular to the backrest of the examination table. The distance between the infrared camera and the sternum of the patients was approximately 2.2 m, while the relative height of the infrared camera with respect to the sternum of the patients was approximately 1.7 m.

B. Marker sets

Before image sequence acquisition, we glued on the skin of the patients, by means of biocompatible gel, a set of wooden spherical markers (5 mm in diameter) consisting of: a) 18 light-colored markers, used to obtain “fiducial points”, i.e., contrasted features for registration; b) 9 dark markers, used as “test points” that do not belong to the registration set, to evaluate the goodness of the registration itself. An example of marker positioning is reported in figure 1a.

Registration was performed using five different sets of fiducial markers, consisting of 18, 12, 9, 7, 5 markers respectively. The test marker set did not change in the five trials considered.

Figure 1 shows the marker sets. The steps followed for positioning the 9-marker set (Fig. 1c) are described below:

I. identify the jugular notch and the infrasternal angle. On the line connecting them, locate point A at 1/3 and point B at 2/3 from the jugular notch, respectively. Apply a marker in B (marker 1);
II. apply a marker on each breast, at the intersection between the medioclavicular line and the transverse axis passing through A (markers 2 and 3);
III. apply a marker on each breast in a lateral position, along the transverse axis passing trough B (marker 4 and 5);
IV. apply a marker at the inferior border of each breast (marker 6 and 7) along the medioclavicular line;
V. apply a marker on each breast in a central position (markers 8 and 9), at the intersection between lines connecting markers 1-4 and 2-6 on the right breast and lines connecting markers 1-5 and 3-7 on the left breast.

Test (dark) markers are added midway between the central and the outer markers. An additional test marker is placed on the sternum on point A.

The sets with 12 markers and 18 markers are obtained from the 9-marker set by adding a marker on the sternum, midway between A and B, and adjunctive markers on the breast contour, as shown in Fig. 1b and Fig. 1a respectively.

The set with 7 markers is obtained again from the 9-marker set, by removing the central markers (see Fig. 1d). Finally, the lateral markers are removed to obtain the 5 marker-set (see Fig. 1e).

C. Realignment of thermograms: the registration algorithm

To compensate movement artifacts we realign the thermograms of the infrared sequences with respect to the first frame, chosen as reference. The first step in any feature-based registration algorithm [8] is the correct detection of the fiducial points used to compute the geometrical mapping and, if needed, of test points used for the evaluation of the registration procedure.

We implemented an algorithm for the localization of the fiducial and test points which segments the

markers in each frame, calculates the centroid of each marker and labels it. After fiducial point localization, the second step is the choice of a suitable transformation for the geometrical matching of the thermograms of the sequence. We chose a piece-wise linear transformation based on the Delaunay triangulation [11] of the selected fiducial points, as it is reported to give good results when small geometric differences between the images to be registered are expected [12], as in this case. Figure 2 shows an example of the triangulation used.

D. Registration evaluation: estimation of the signal-to-noise ratio improvement

After the thermograms of the sequence have been realigned by means of the described algorithm, it is important to evaluate the performance of the algorithm itself. Usually, in the literature describing marker-based image registration approaches, this evaluation is provided estimating the alignment error [8], i.e. the test points residual mismatch among the reference frame and the realigned frames [13].

However, in the analysis of biomedical infrared image sequences, the simple consideration of this alignment error is not satisfactory. In fact, it does not provide quantitative information on the quality of the temperature variations vs. time signals related to a certain skin portion. To overcome this problem, we introduced a model [7] that allows a quantitative estimation of the signal-to-noise ratio increase after the thermal images of the sequence have been realigned. Considering a small portion of skin and indicating by $T(x,y,t)$ the temperature that the infrared sensor measures in the point (x,y) at a given time instant t, temperature variations in time captured by the infrared camera are a combination of the physiological variations of the skin temperature (the signal of interest) and of apparent temperature changes actually due to patient's movements (noise).

The total derivative of temperature with respect to time, dT/dt, is:

$$\frac{dT}{dt} = \frac{\partial T}{\partial t} + \frac{\partial T}{\partial x}\frac{\partial x}{\partial t} + \frac{\partial T}{\partial y}\frac{\partial y}{\partial t} = \frac{\partial T}{\partial t} + (\vec{v} \cdot \nabla)T, \qquad (1)$$

where $\vec{v} = (v_x, v_y)$ is the 2-dimensional velocity of the skin portion and ∇T is the spatial temperature gradient. Equation 2 reports the expression of the noise $N(x, y, t)$ introduced by motion artifacts.

$$N(x, y, t) \approx \int_0^t \vec{v}(x, y, t') \cdot \nabla T(x, y, t') dt' \qquad (2)$$

The signal-to-noise ratio of the process - at each point *(x,y)* - is defined as $S/N \equiv \sigma_T^2(x, y) / \sigma_N^2(x, y) - 1$, where σ_T^2 (x,y) is the variance of the measured temperature time series *T(x,y,t)* (signal plus noise) and $\sigma_N^2(x, y)$ is the variance of the noise, as given by Eq. (1). Similarly, we define the signal-to-noise ratio after registration as $(S/N)_R \equiv \sigma_{T_R}^2(x, y) / \sigma_{N_R}^2(x, y) - 1$, where $\sigma_{T_R}^2(x, y)$ is the variance of the measured temperature time series $T_R(x,y,t)$ obtained after sequence realignment and $\sigma_{N_R}^2(x, y)$ is the variance of the term $\int_0^t \vec{v}_R(x, y, t') \cdot \nabla T_R(x, y, t') dt'$, being $\vec{v}_R(x, y, t)$ the residual velocity, not compensated by the registration algorithm.

E. Data processing

For each subject we realigned the thermal images of the sequence using the five markers sets described above. We calculated the instantaneous velocity of test points before and after registration. We obtained the instantaneous velocity at each pixel using a nearest neighbor interpolation scheme [7]. Using Eq. 1, we estimated the signal-to-noise ratio increment due to registration for each of the five different sets of fiducial markers, at each image pixel. Finally, we calculated the mean of the signal-to-noise ratio increment over the entire breast (markers excluded), for each trial. We demonstrated that the signal-to-noise ratio is estimated with an uncertainty of 0.25 dB [7].

III. RESULTS AND DISCUSSION

The time required to prepare the patients varies approximately from 5 minutes for the 5-marker set to 15 minutes for the 18-marker set. Since our objective was to compare the performance of the different marker sets, in the following we report the *increment* of the signal-to-noise ratio after the registration, (i.e. the signal-to-noise ratio of the registered sequence minus the signal-to-noise ratio of the raw sequence). To have a measure of the quality of the realigned sequence, only its signal-to-noise ratio is to be considered.

Figure 3 shows the signal-to-noise ratio increment after registration with the 18, 12, 9, 7 and 5 marker sets. The twenty-subject sample population was divided among small, medium, and large breast size subjects, basing the classification on the chest measure and cup size.

In all cases there is a decrease of the performance of the registration algorithm using a smaller number of fiducial markers (2dB in the worst case). The small and medium breast size samples show similar trends: the S/N improvement after registration increases using more markers, up to the 12-marker set. Then, there is no further improvement using the 18-marker set. The large breast size sample shows a slightly different trend and lower S/N increments for all marker sets.

These results demonstrate that 18, 12 or 9 marker sets give a very similar increment of the signal-to-noise ratio, while 5- and 7-marker sets are clearly less effective.

This is confirmed by pair-wise, one-tail, Student's t-test applied to the twenty-subject sample: the 12-marker set does not give results statistically different from those obtained by the 18-marker set (p-value > 0.15). Performances of the 9-marker set are slightly worse than those of the 12-marker set ($p = 0.002$), while the 7-marker and 5-marker sets performances are significantly different from those of the 12-marker set ($p < 0.0001$).

IV. CONCLUSION

We compared the performance of five different marker sets used to obtain motion artifact reduction and

signal-to-noise ratio improvement of infrared thermal sequences to be used in early breast cancer detection and follow-up. We demonstrated that a set consisting of 12 markers gives results that are statistically equivalent to those given by the 18-marker set. Further reducing the number of markers to 7 or 5 causes a statistically significant reduction of the signal-to-noise ratio improvement.

In conclusion, we believe that the 9-marker and 12-marker sets herein described are a good compromise between simplicity and the need for an effective motion artifact reduction in the clinical practice as well as in research.

ACKNOWLEDGMENT

This work was supported by the Fondazione CRT (Torino, Italy) in the research framework of the Clinical Industrial Research Park Foundation (Torino, Italy).

REFERENCES

[1] M. Anbar, L. Milescu, A. Naumov, C. Brown, T. Button, C. Carty and K. AlDulaimi, “Detection of Cancerous Breasts by Dynamic Area Telethermometry”, *IEEE Eng. Med. Biol.*, vol. 20, pp. 80–91, Sept./Oct. 2001.

[2] M. Anbar, C. Brown, L. Milescu, L. Babalola and L. Gentner, “The potential of dynamic area telethermometry in assessing breast cancer”, *IEEE Eng. Med. Biol.*, vol. 19, pp. 58–62, Mar./Apr. 2000.

[3] T. M. Button, H.. Li, P. Fisher, R. Rosenblatt, K. Dulaimy, S. Li, B. O’Hea, M. Salvitti, V. Geronimo, C. Geronimo, S. Jambawalikar, P. Carvelli and R. Weiss, “Dynamic infrared imaging for the detection of malignancy”, *Phys. Med. Biol.*, vol. 49, pp. 3105–3116, Jul. 2004.

[4] S. R. Fanning, S. Short, K. Coleman, S. Andresen, G. T. Budd, H. Moore, A. Rim, J. Crowe and D. E. Weng, “Correlation of dynamic infrared imaging with radiologic and pathologic response for patients

treated with primary systemic therapy for locally advanced breast cancer", *Journal of Clinical Oncology, 2006 ASCO Ann. Meeting Proc. (Post-Meeting Edition)*, vol 24, no. 18S.

[5] M. A. Fauci, R. Breiter, W. Cabanski, W. Fick, R. Koch, J. Ziegler, and S. D. Gunapala, "Medical Infrared Imaging – differentiating facts from fiction, and the impact of high precision quantum well infrared photodetector camera systems, and other factors, in its re-emergence", *Infrared Phys. And Tech.*, vol. 42, pp. 337–344, Jun. 2001.

[6] K. R. Foster, "Thermographic detection of breast cancer", *IEEE Eng. Med. Biol.*, vol. 17, pp. 10–14, Nov./Dec. 1998.

[7] V. Agostini, S. Delsanto, F. Molinari, M. Knaflitz, "Noise estimation in infrared image sequences: a tool for the quantitative evaluation of the effectiveness of registration algorithms", *IEEE Trans. Biomed. Eng.*, to be published.

[8] B. Zitova and J. Flusser, "Image Registration Methods: a Survey", *Image and Vision Computing*, vol. 21, pp. 977–1000, Oct. 2003.

[9] C. L. Herry, "Segmentation and Landmark Identification in Infrared Images of the Human Body", in *Proc. 28th IEEE EMBS Ann. Int. Conf.*, New York, USA, 2006, pp. 957–960.

[10] N. Scales, C. Herry, M. Frize, "Automated Image Segmentation for Breast Analysis Using Infrared Images", in *Proc. 26th IEEE EMBS Ann. Int. Conf.*, San Francisco, CA, USA, 2004, pp. 17371740.

[11] A. Goshtasby, "Piecewise linear mapping functions for image registration", *Pattern Recognition*, vol. 19, pp. 459–466, 1986.

[12] L. Zagorchev, and A. Goshtashby, "A Comparative Study of Transformation Functions for Nonrigid Image Registration", *IEEE Trans. Image Proc.*, vol. 15, no. 3, pp. 529–538, 2006.

[13] V. Agostini, S. Delsanto, F. Molinari, M. Knaflitz, "Evaluation of feature-based registration in dynamic infrared imaging for breast cancer diagnosis", in *Proc. 28th IEEE EMBS Ann. Int. Conf.*, New York, USA, 2006, pp. 953–956.

Figure captions

Figure 1.

The five different skin marker sets used for registration. From top to bottom: (a) 18-marker set; (b)12-marker set; (c) 9-marker set and its construction; (d) 7-marker set; (e) 5-marker set. Light-colored markers are fiducial markers, while dark-colored ones are test markers.

Figure 2.

Single thermal frame extracted from the infrared sequence of the subject shown in Figure 1: Delaunay triangulation is shown superimposed for the 9-marker set.

Figure 3.

Increment of the signal-to-noise ratio due to registration respectively with 18, 12, 9, 7 and 5 markers (mean ± 1 standard error).

Figure 1

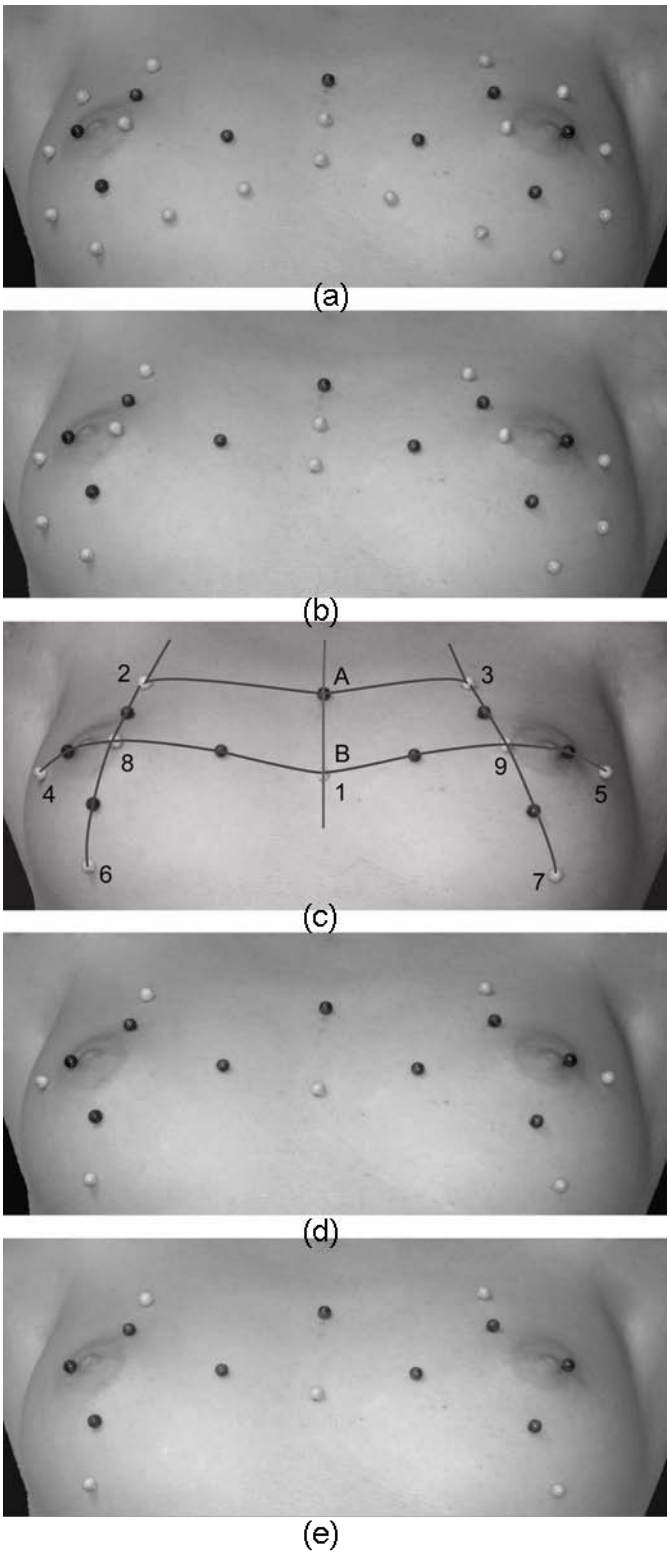

Figure 2

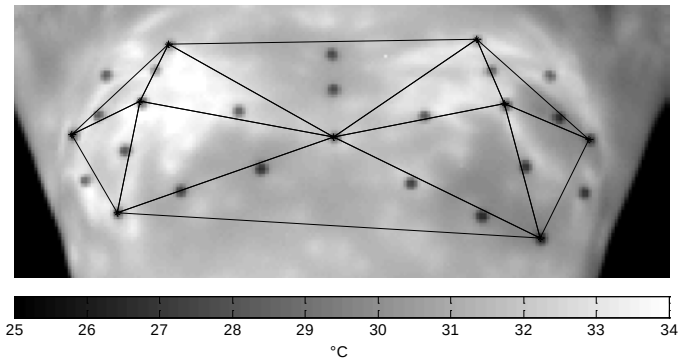

Figure 3

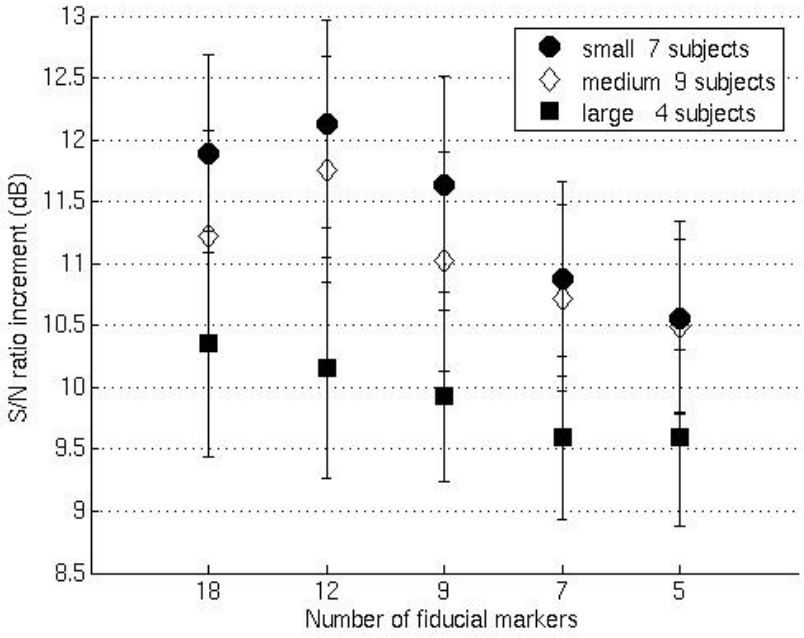
small 7 subjects
medium 9 subjects
large 4 subjects
S/N ratio increment (dB)
13
12.5
12
11.5
11
10.5
10
9.5
9
8.5
18
12
9
7
5
Number of fiducial markers